Closed loop control of a flap exposed to harmonic aerodynamic actuation

Velte, Clara Marika; Mikkelsen, Robert Flemming; Sørensen, Jens Nørkær; Kaloyanov, Teodor ; Gaunaa, Mac

Published in:
Proceedings of Torque 2012, The science of making torque from wind

Publication date:
2012

Closed loop control of a flap exposed to harmonic aerodynamic actuation

C M Velte[1], R Mikkelsen[1], J N Sørensen[1], Teodor Kaloyanov and M Gaunaa[1]
[1] Department of Wind Energy, Technical University of Denmark, 2800 Kgs. Lyngby, Denmark

E-mail: cmve@dtu.dk

Abstract. Wind tunnel testing of a two-dimensional aerofoil with a load reducing flap has been conducted under the influence of a closed-loop controller (PID). Upstream synthetic perturbations for well-defined testing of the controller were generated by instrumenting the wind tunnel with two fast turning vanes placed in front of the main test wing. These were situated symmetrically above and below the airfoil in a way that created a fast turning of the air flow without directly affecting the boundary layer on the test airfoil. The Reynolds number was Re=500.000. The PID-controlled flap was able to alleviate the load variations with reductions above 80% for reduced frequencies up to k = 0.028 and nearly 70% at k=0.054. At about 0.108 and higher a different strategy is needed for the present setup as the reduction is low or even negative.

1. Introduction

Wind turbine blades with flaps for gust alleviation and reducing other fast changes, e.g., half wake loads, has matured to a level where full scale testing is being carried out [1]. Combined designs of blades with flaps are, however, still in its infancy for new turbines on the market. Long term testing is needed but also basic 2D aerofoil testing is valuable for choosing flap, actuations and sensor for an actual blade design. Wind tunnel testing of two-dimensional airfoils with load reducing devices has been conducted by many, e.g., using flap designs based on piezo-actuated [2,3], mechanically hinged, flexible vs. stiff flaps. Numerical CFD analysis has been conducted on micro-tabs [4] but also on piezoelectric [5] benders mounted as TE flaps. Bak et al. [2] showed that aerodynamically they could reduce loads by 60-80% at relevant reduced frequencies; however, several challenges still remain for practical implementations of the piezo-actuator on a real blade due to the sensitive nature of this device.

Testing closed loop controller behavior the method preferred by most has been to pitch or move the 2D wing harmonically by a mechanism and then alleviate the changes with the flap. Here it is proposed to generate fast turning of the airflow with moderate amplitude passing by the test wing. One way to accomplish this is to instrument the wind tunnel with dynamically suspended vanes or symmetrical wings placed upstream of the main wing, here connected to a motor driven eccentricity mechanism. A schematic drawing of the tunnel configuration is shown in Figure 1. The proposed setup has been established in the test section at DTU-MEK's 0.5x0.5m^2 low speed wind tunnel for closed loop controller testing. The main wing (NACA 64418 aerofoil, c=0.25m) was designed with a 15% flexure type suspended flap, actuated using an internally mounted linear motor connected to a rudder horn on the pressure side and fitted with pressure tabs around the foil.

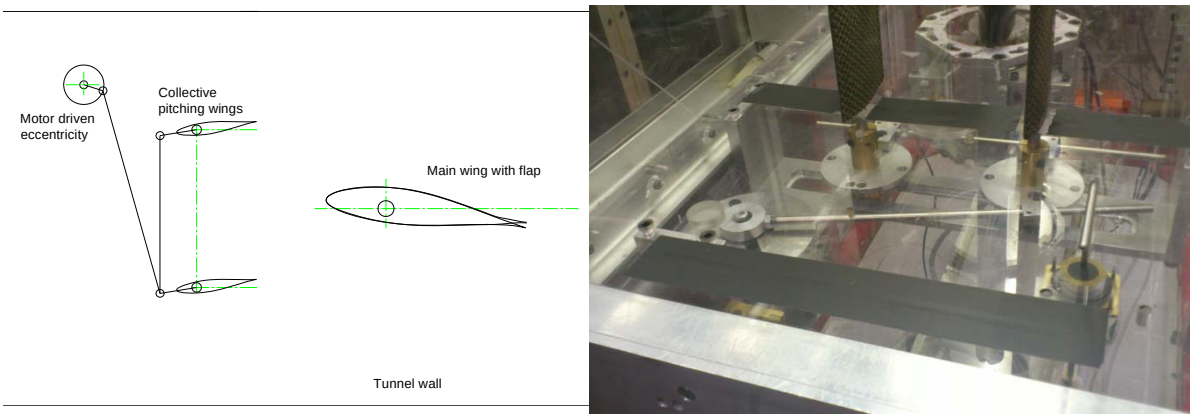

Figure 1 Tunnel configuration with upstream pitching wings and main wing with controllable trailing edge flap, left, developed mechanism mounted in tunnel test section, right.

The combined chain of measurement comprised pressure scanner signals (63 on foil, 1 for tunnel dynamic pressure), flap actuation, main wing pitch in a closed loop control (PID) environment with about 100 Hz frequency updating. For the present campaign the Reynolds no was set to Re=500.000.

2. Experimental method

The test airfoil is mounted in a wind tunnel, attached to a pitch mechanism controlled with an AC servo motor. In order to measure the airfoil load, the wing was fitted with 63 pressure tabs located on the surface of the airfoil. To ensure a fast response, the tabs were connected to pressure scanners mounted inside the wing resulting in short tubing length of about 20 cm. A LabView user interface was developed handling combined readings from the pressure tabs, tunnel speed, etc. serving to compute the wing loads. The integrated loads serve to control the flap motor using analogue voltage signals. The computer/hardware interface was achieved using a *NI-DAQ* card.

2.1. Wind tunnel

An open loop suction wind tunnel is used as a basis for the control setup. The test section has a cross section of 0.5 m x 0.5 m for testing, length 1.4 m, contraction ratio 12.5:1 and a maximum wind speed of 60 m/s. The turbulence intensity is about TI = 0.08-0.07, which is low enough for natural transition to develop. The tunnel flow quality is adequate for airfoil investigation and mainly limited by the highest achievable Reynolds number ($>10^6$) and the chord to tunnel aspect ratio (1:2). Based on the above, the overall system accuracy is considered to be accurate enough to serve the purpose of testing closed loop control of a wing with a flap.

2.2. Model wing with flap

A NACA64418 aerofoil section was chosen for the main wing as this is a common foil used for wind turbine blades and it has been the subject of other studies. The airfoil section was constructed from carbon fiber molded to the subscribed shape. The airfoil had a mechanical frame made out of aluminum ribs and a flexible trailing edge flap with thinner fiber sections in the surface at the bending positions for a continuous airfoil surface. The design aims at a 15% flap for a wing section of 250 mm, i.e., 37.5 mm. Figure 2, the *e+s* section on the rear suction side is the flexible part, however, with the bending happening within the *e*-section and with the *s*-section considered to be stiff. The overlap region is marked as the *o*-section. The flap actuation was provided through a LinMot P01-23Sx80/30x90 linear motor.

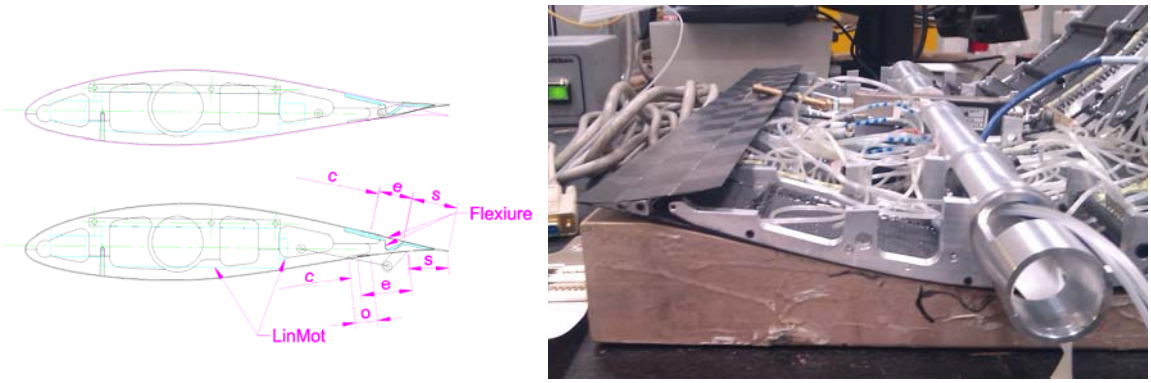

Figure 2 NACA 64418 model wing with flap

The LinMot was in turn mastered by an E1100-GP-HC controller receiving instructions from a computer through the LabView user interface.

The actuation of the flap is done through a rudder horn on the pressure side, designed such that a slider movement of ±8 mm results in a change of ±16° flap angle. The accuracy of the position is initially 0.1 mm using only the slider as sensor, but could be improved with an additional optical sensor which may reduce position uncertainty to less than 0.01mm. For the present campaign only the slider has been used. The mass of the slider is 89g and the mass of the flap parts is less than 50 g. Thus, the main part of the force serves to balance the flexible forces and the aerodynamic loads. The actuator can deliver a peak force of 39 N and continuous RMS force of 14 N.

A JVL AC-servo motor is used to control the pitch movement/position/AOA of the test wing through a worm wheel gear (1:25) mechanism. The power/analog input is connected to the *NI-DAQ* unit handling the voltage signal generated via the *LabView−VI*. The connection between the PC and the servo motor is realized using a digital *COM* cable.

2.3. Pressure measurement system

In order to capture the pressures on the surface of the airfoil, a system from Esterline Pressure Systems, PSI is used. A central *DTC−Initium* unit is connected to two electronic 32HD Miniature Pressure Scanners, each with 32 ports having a measuring range of ±7000Pa and ±2500Pa. The scanner with high range pressure capability measures the pressure on the suctions side of the airfoil, while the low range scanner measures on the pressure side of the airfoil for improved dynamic range. The surface pressures measured with the PSI scanners have an accuracy of ±0.05% of full scale, equivalent to ±2.5Pa. The pressure scanners are connected to the tabs with short plastic tubing (~ 20 cm) and the tabs which are not connected are blocked with a small dead-end tube. The interface cables of the linear motor and the pressure scanners, along with the static reference pressure, are connected through the main support beam of the wing to the *DTC−Initium* pressure unit and LinMot controller.

The model wing is instrumented with pressure tabs in line located at three spanwise sections, 17%, 41% and 68% span. Tabs are normally not in line on 2D foils, however, due to space constrains and requirements for the linear motor, diagonally positioned tabs were not feasible. All three sections were used for initial measurements testing the two-dimensionality of the flow. The outcome showed good agreement between the sections although with expected changes towards the wall at 17% span. The subsequent testing was carried out using the 41% span, with the flap being actuated at 50% span.

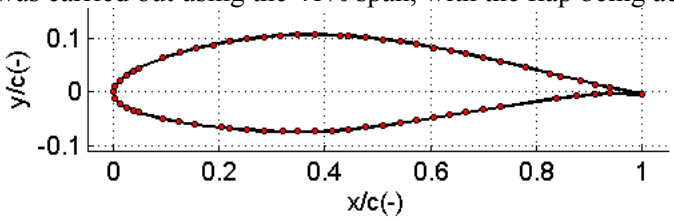

Figure 3 Pressure tabs on NACA 64418 model wing. No tabs in overlapping region at the rear on the pressure side

The scan rate was set to 100 Hz (could be as high as 20kHz/No. of tabs), with an Ethernet connection ensuring rapid communication between the pressure measuring system and the computer LabView interface which also controls the linear actuator motor.

2.4. Aerodynamic forcing – oscillating wings

In order to perform closed loop control testing, two oscillating wings connected to a mechanism for fast harmonic pitch movement were positioned upstream of the main wing. The main idea is to apply air turning of the flow approaching the test wing such that the disturbance frequency can be controlled with high accuracy. The resulting change in effective angle of attack leads to changed forces later to be canceled out by the control flap on the main wing. The usual approach applied by most has typically been to pitch or move [6] the test wing rather than changing the flow direction. Frederick et al. [7] used a square/bluff body in-line with the test aerofoil resulting in von Karman type wake flow sheeting Strouhal frequency dependent disturbances. In that perspective the present approach is considered to open up for new possibilities for open loop controller testing of wings with flaps. Positioning the upstream wings so that they are not in line with the main wing ensures that the boundary layer generated wake from the oscillating wings is not affecting the main wing boundary layer to develop by its own. The construction allows for adjusting the amplitude of the pitching moment directly through the eccentricity mechanism. The actual magnitude of the forcing is in the present setup not known, but at first considered to be lees important although it should be of a magnitude clearly affecting the main wing. The two wings are configured to oscillate synchronously through a bar connecting the two. A stepper motor sets the frequency of the desired oscillations presently controlled manually using an electronic sine generator.

2.5 Uncertainty aspect

Estimation of the wing pitch accuracy from repartition tests sets the uncertainty to ±0.5° mainly due to manual setting of zero AOA. The linear motor has with the current setting a position uncertainty of ±0.1 mm corresponding to ±0.2° for the flap angle. This could be improved with an additional optical sensor; however, the size of the wing does not allow for this at present. The wing is made from a CNC milled mould with high accuracy.

The complete set of pressures recorded by the pressure measurement system was read into a LabView VI. Further, the target position of the flap and the static pressure for determining the wind tunnel speed were read into the program. The same VI was used to compute the integrated lift coefficient and subsequently used this as input for a simple PID controller to control the LinMot actuating the flap. These signals were all plotted and monitored in real-time and could readily be exported for further processing using separate software.

A separate VI was responsible for controlling the linear actuator motor when the PID controller was not in use as well as the pitching motor of the main airfoil.

3. Results

Three sets of experiments have been conducted:

- Static testing - flap variations through an AOA range
- Harmonic flap variation
- Closed loop control with upstream aerodynamic forcing

In order to limit parameter variations, the experiments were carried out at a tunnel speed of 30 m/s, equivalent to $Re=5\cdot10^5$. The sampling rate was 100 Hz. Data was always collected for a time period of 15 s.

3.1. Static measurements

Measurements of the static response was conducted for AOA α = 0°, 5°, 7°, 10° and flap angles β = −9°, −6°, −3°, 0°, 3°, 6°, 9°. Figure 4 left, presents the pressure distribution in usual graphical form at α = 6°. The flow at this AOA is attached. The stagnation pressure level of C_p = 1 is observed in the LE indicating the level of normalization is of the right order.

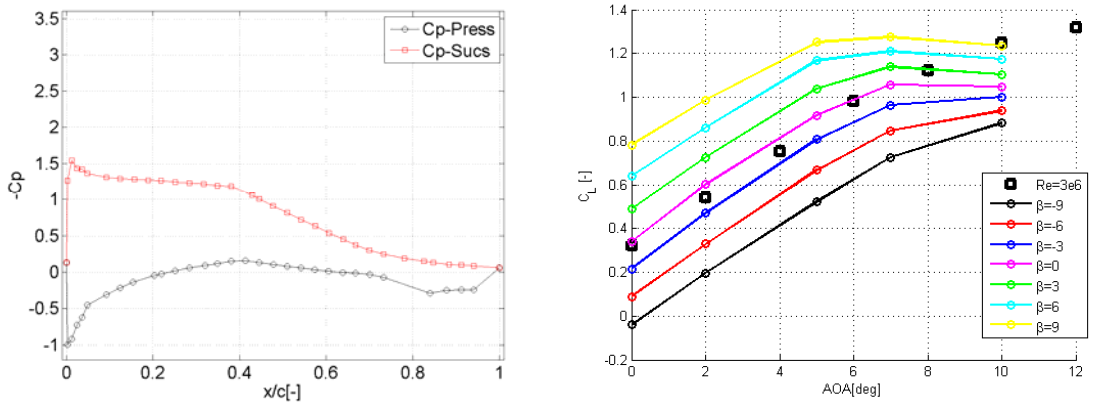

Figure 4 pressure distribution, AOA=6°, left. Lift vs. AOA and flap beta, static.

The LE pressure is assumed to be the arithmetic mean of the two nearest pressures, since it was impossible for practical reasons to place a tab at the LE point. The integral lift changes are shown in Figure 4, right. The dynamic range of the flap is approximately measured to $\Delta C_L \approx \pm 0.4$ in the attached regime for static flap deflection of $\beta = \pm 6°$. Result for $\beta = \pm 3, 9°$ are also shown and even higher dynamic ranges could be achieved with the present flap design. Inserted are also high Re no. measurements [8] showing a reasonable comparison in the linear regime, with separations occurring earlier ($\alpha \approx 7°$) as expected at the lower Re presently used.

3.2. Harmonically oscillating flap

In order to picture the achievable dynamic range of the flap exposed to harmonic actuation, measurements were performed considering forced harmonic movement of the flap at reduced frequencies within the range k=0.02-0.21 and flap deflections of $\Delta\beta = 2.5°, 5°, 10°$.

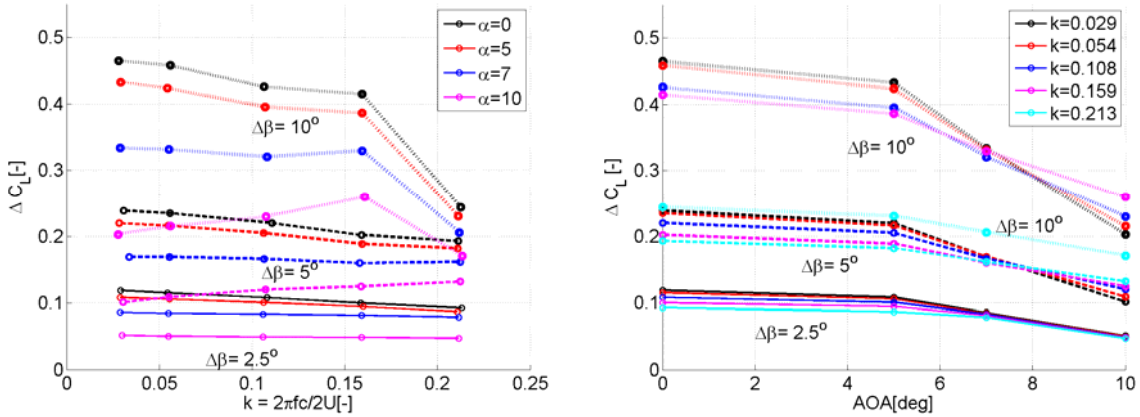

Figure 5 Dynamic range of flap, ΔC_L vs. AOA and reduced frequency k. Full lines $\Delta\beta=2.5°$, dashed lines $\Delta\beta=5°$ and dotted lines $\Delta\beta=10°$.

Figure 5 left, shows obtainable ΔC_L by changing the reduced frequency $k = 2\,\pi\, f\, c/2U$ at AOA=0,5,7 and 10°. Figure 5 right, presents the same data interchanging reduced frequency and AOA. The setup is well capturing the limits of expected trends showing the reduced flap performance in terms of ΔC_L towards higher reduced flap frequency and stall AOA.

3.3. Closed loop control

For controlling the flap a simple PID algorithm was employed with the fully integrated lift obtained from all the active pressures tabs. As controlled disturbance, the upstream positioned vanes were set to pitch harmonically trough the above mentioned mechanism. Using the fully integrated lift from all tabs is on a real turbine blade unrealistic, but in a tunnel experiment it may serve as reference for other strategies pursued. One such strategy which could be realized on a real blade, is measuring a single pressure difference strategically which is discussed later.

3.4. Full integrated lift

Figure 6 left, shows the reduction in ΔC_L with and without control. It is seen that the disturbance from the oscillating wings are of the order ΔC_L =0.1, which is a reasonable level to alleviate the flap control. The instantaneous integrated lift, based on the 63 pressure tabs, is used as the process variable for the controller. *PID* gains were tuned at AOA = 7° and k = 0.108 manually with P = 0.95, I = 0.00008 and D = 0.000006. These can most probably be improved using common gain determination strategies. Despite the crude gain tuning, the controller is seen to reduce the loads significantly at reduced frequency k = 0.028 and 0.054, but fails completely at k = 0.158. At k = 0.108 only limited reduction is seen. Reductions above 80% are obtained, figure 6 right, at a lower reduced frequency of k=0.028 and nearly 60% at k=0.054. At about 0.108 and higher a different strategy is needed for the present setup as the reduction is low or even negative.

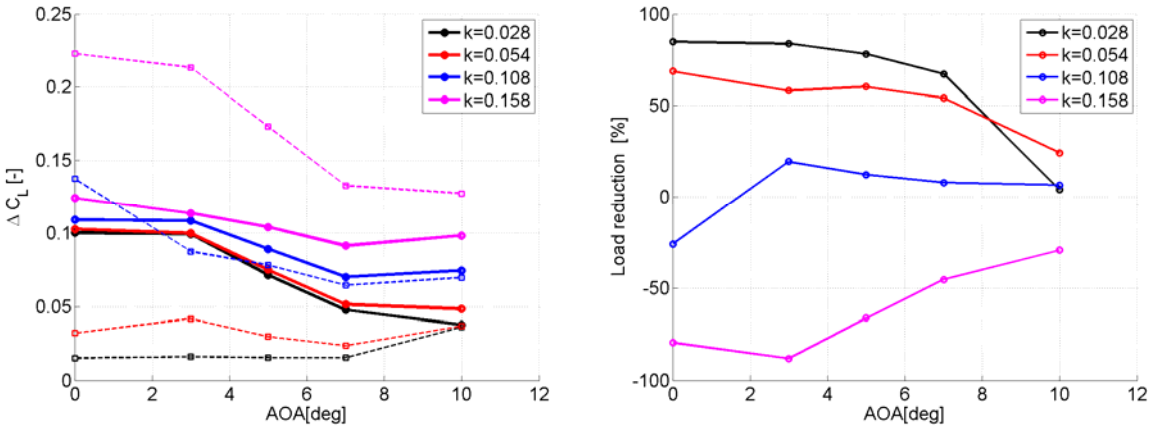

Figure 6 Reduction in ΔC_L, left, dotted lines with control, full lines without. Load reduction in %, right.

Thus, the setup has the capability to accurately test load reductions at specified reduced frequencies and furthermore push the controller to the limits of where it may not work.

3.5. 2-point pressure difference

Other control strategies should be pursued since the full pressure distribution only may serve as reference, e.g., as using a pressure difference near the LE as done by Gaunaa and Andersen [9]. The model of Gaunaa and Andersen suggest through linearization that

$$C_L = \frac{L}{\frac{1}{2}\rho V^2 c} = K_c \alpha_{c,eff} + K_{\dot{\alpha}} \frac{\dot{\alpha} c}{V} + \underbrace{K_L\left(\ddot{y}, \ddot{\alpha}, \dot{\beta}, \ddot{\beta}\right)}_{HO} \approx \frac{\partial C_L}{\partial \alpha}\left(\alpha_{c,eff} - \alpha_o\right) + K_{\dot{\alpha}} \frac{\dot{\alpha} c}{V} \qquad (1)$$

and that a local pressure difference be given as

$$C_p = \frac{\Delta p}{\frac{1}{2}\rho V^2} = g_c(x)\alpha_{c,eff} + g_{\dot{\alpha}}(x)\frac{\dot{\alpha} c}{V} + g_\beta(x)\beta + g_{camber}(x) + \underbrace{g_L\left(\ddot{y}, \ddot{\alpha}, \dot{\beta}, \ddot{\beta}\right)}_{HO} \qquad (2)$$

Neglecting higher order terms and using a result from thin airfoil theory that $g_{\dot{\alpha}}(x) = 0$ at 12.5% x/c, the effective AOA can be derived as

$$C_p = \frac{\Delta p}{\frac{1}{2}\rho V^2} = K_1 \alpha_{c,eff} + K_2 \beta + K_3 \quad \Rightarrow \quad \alpha_{c,eff} = \frac{1}{K_1}\left[\frac{\Delta p}{\frac{1}{2}\rho V^2} - K_2 \beta - K_3\right] \qquad (3)$$

to be inserted in Eq. (1) for estimation of C_L. The constant $K_1, K_2, K_3, \alpha_o, \partial C_L/\partial \alpha$ may be derived from static measurements by varying the AOA and the flap angle, here found to be K_1=*0.24*, K_2=*-0.04*, K_3=*0.3*, α_o=*-3°*, $\partial C_L/\partial \alpha = 0.107$, Prior to using the 2 point pressure difference as control variable the model may be evaluated directly based on the constants derived. Figure 7 displays measured sectional lift coefficient, 2-point pressure difference and estimated lift based on this at AOA=4° and reduced frequency k=0.054 and 0.158.

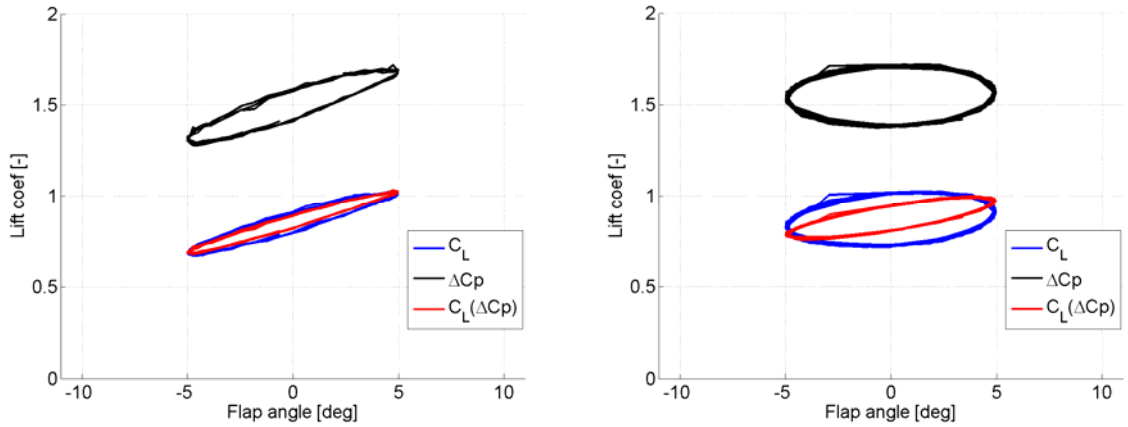

Figure 7 Lift vs. flap at reduced frequency k=0.054, left, and k=0.158 right.

At moderate values of reduced frequency the prediction is good but not perfect whereas at the high value the difference appears high. Considering possible explanations some remarks can be referred to that

- The airfoil was thick (0.045 m) compared to the test section cross section (0.5 m), meaning that the tests suffered a certain amount of blockage (9%).
- The thin airfoil theory, on which the theory is based, assumes thin airfoils and infinite Reynolds numbers.
- Higher order terms that are neglected in the theory may not be negligible in the present case.
- Errors in the determination of constants for estimating the lift from the theory

Presently, the 2 point pressure difference has not been applied as control variable in the current setup, but is to be pursued in future work.

Summary and conclusions

A new setup for testing trailing flaps on an aerofoil in a wind tunnel has been developed for a closed loop controller testing. Upstream wings connected to a fast pitching mechanism were developed serving to apply harmonic loads to the test wing. The main wing is thereby excited with a well defined frequency and the capability of the flap control can accurately be tested with respect to load reduction and limits of use. Measurements on a NACA64418 aerofoil at Re=500.000 and reduced frequencies k=0.02-0.2 were conducted. Load reductions up 80% were found at k=0.028, reducing with increasing values of k and subsequently failing to reduce at tested values k>0.11 with the applied control strategy.

Acknowledgments

The work is part of the Danish ATEF-project funded by Danish High Technology Foundation (Højteknologifonden)

References

[1] Castaignet, D. Model predictive control of trailing edge flaps on a wind turbine blade. PhD thesis, DTU, 2011.
[2] Bak C, Gaunaa M, Andersen PB, Buhl T, Hansen P, Clemmensen K, Moeller R. Wind tunnel test on wind turbine airfoil with adaptive trailing edge geometry. 45th AIAA/ASME 2007; 8:12314-12325
[3] Andersen PB. Advanced load alleviation for wind turbines using adaptive trailing edge flaps: Sensoring and control. PhD Thesis, DTU, 2010.
[4] Chow R, van Dam CP. Computational investigation of small deploying tabs and aerodynamic load control. J. Physics: Conf. Series 2007; 75:012080
[5] Heinz J, Sørensen NN, Zahle F. Investigation of load reduction potential of two trailing edge flap controls using CFD. Wind Energy 2011; 14:449-462
[6] Gaunaa M. Unsteady Aerodynamic Forces on a NACA 0015 Airfoil in Harmonic Translatory Motion. PhD Thesis, DTU, Denmark, April 2002
[7] Frederick M, Kerrigan EC, Graham JMR. Gust alleviation using rapidly deployed trailing-edge flaps. Jour. Wind Eng. and industrial aerodynamics, 98:712-723, 2010.
[8] Abbott IH, von Doenhoff, AE. Theory of Wing Sections: Including a Summary of Airfoil Data. Dover Publications, 1959
[9] Gaunaa M and Andersen PB. Load reduction using pressure difference on airfoil for control of trailing edge flaps. In 2009 European Wind Energy Conference and Exhibition, 2009, Marseille (FR), 16-19 Mar, 2009.